The SNR W28 at TeV Energies

G.P. Rowell[1], T. Naito[2], S.A. Dazeley[3], P.G. Edwards[4], S. Gunji[5], T. Hara[2], J. Holder[1], A. Kawachi[1], T. Kifune[1], Y. Matsubara[8], Y. Mizumoto[9], M. Mori[1], H. Muraishi[10], Y. Muraki[8], K. Nishijima[7], S. Ogio[6], J.R. Patterson[3], M.D. Roberts[1], T. Sako[8], K. Sakurazawa[6], R. Susukita[11], T. Tamura[12], T. Tanimori[6], G.J. Thornton[3], S. Yanagita[10], T. Yoshida[10] and T. Yoshikoshi[1]

[1] *Institute for Cosmic Ray Research, University of Tokyo, Tokyo 188-8502, Japan*
[2] *Fac. of Management Information, Yamanashi Gakuin University, Yamanashi 400-8575, Japan*
[3] *Dept. of Physics and Math. Physics, University of Adelaide 5005, Australia*
[4] *Institute of Space and Astronautical Science, Kanagawa 229-8510, Japan*
[5] *Dept. of Physics, Yamagata University, Yamagata 990-8560, Japan*
[6] *Dept. of Physics, Tokyo Institute of Technology, Tokyo 152-8551, Japan*
[7] *Dept. of Physics, Tokai University, Kanagawa 259-1292, Japan*
[8] *Solar-Terrestrial Environment Lab., Nagoya University, Aichi 464-8601, Japan*
[9] *National Astronomical Observatory of Japan, Tokyo 181-8588, Japan*
[10] *Faculty of Science, Ibaraki University, Ibaraki 310-8512, Japan*
[11] *Institute of Physical and Chemical Research, Saitama 351-0198, Japan*
[12] *Faculty of Engineering, Kanagawa University, Kanagawa 221-8686, Japan*

Abstract. The southern supernova remnant (SNR) W28 was observed in 1994 and 1995 by the CANGAROO 3.8m telescope in a search for multi-TeV gamma ray emission, using the Čerenkov imaging technique. We obtained upper limits for a variety of point-like and extended features within a $\pm 1^\circ$ region and briefly discuss these results, together with that of EGRET within the framework of a shock acceleration model of the W28 SNR.

INTRODUCTION

W28 is a composite SNR (mixed or M-type) with centrally filled X-ray and optical emission and limb brightened or shell-like radio emission [10,6]. It lies at a distance of about 1.8 kpc (from Σ-D, although kinematic arguments place a higher figure of 4 kpc), has an age of between 3.5-15$\times 10^4$ yrs, and evolution consistent with the radiative or Sedov phases. The radio shell ($\sim 1^\circ$ diameter) is dominated by the northern half and over 40 maser emission (1720 MHz) sites have been identified indicating strong interaction with a molecular cloud [2]. The

ROSAT X-ray emission is well explained by a thermal model, but recent ASCA data hint at non-thermal emission in the southwest region [13]. A flat spectrum (integral index -0.9) unidentified EGRET source, 3EG J1800-2338 (0.32° 95% error circle radius), [4] is centred on the southern radio edge. W28 and the EGRET source are a strong example of an EGRET source/SNR association [11]. The radio pulsar PSR J1801-23 at the northern SNR edge is not thought to be associated with W28 given the difference in distances of this and the SNR [5].

SNR are thought primarily responsible for the acceleration of galactic cosmic-rays (CR) and W28 is a good southern hemisphere example of such a site. Gamma-ray emission can be produced from one, or a combination of hadronic ($p + p \rightarrow \pi^\circ \rightarrow 2\gamma$) and electronic (inverse Compton boosting of ambient soft photons and bremsstrahlung) processes extending up to TeV energies. The emission at TeV energies (and non-thermal X-ray synchrotron emission) is therefore a tracer of CR acceleration.

DATA ANALYSIS AND RESULTS

We used the 3.8 metre telescope of CANGAROO [3] in a search for TeV gamma-ray emission from the W28 region over two observation seasons (1994 and 1995). The imaging camera on this telescope has a field of view $\sim 3^\circ$ on a side and we have used an analysis that maintains a roughly constant gamma-ray selection power for sources located within a $\sim 1^\circ \times 1^\circ$ area [12] of the telescope tracking position. ON source data were complemented by a set of OFF source data (tracking position displaced in right ascension only) for background comparison. Following removal of data under the influence of weather and instrumental effects, a total (for 1994 and 1995) of 57.5 hours ON and 53.5 hours OFF source data were accepted for analysis.

The image cuts on data are based on a combination of the Hillas image orientation, location and size parameters (see [9] for a technique summary). W28, if a TeV emitter, may contain both point-like and extended features, requiring a detailed study of the off-axis performance of the CANGAROO 3.8m camera. Simulations of the telescope/camera combination reveal a decreasing gamma-ray selection efficiency of the cuts for off-axis point sources, due to camera-edge effects. It is possible to maintain an improved gamma-ray cut efficiency over the camera using a combination of cuts that are dependent on the location of the assumed source. One of these cuts, D, characterises the distance between the assumed and reconstructed source position for each event:

$$D = \sqrt{\left(\frac{miss}{\sigma_{miss}}\right)^2 + \left(\frac{dis - dis_{ex}}{\sigma_{dis}}\right)^2} \qquad (1)$$

where the expected dis of an image, $dis_{ex} = 1.25(1.0 - \frac{width}{length})$, is dependent on the image elongation. The standard deviations are given by $\sigma_{dis} = 0.21 + 0.09d$, ie.

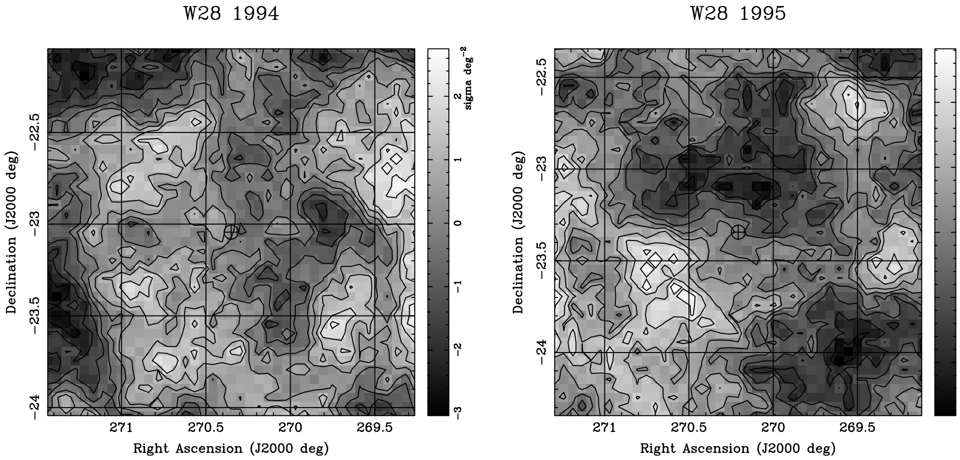

FIGURE 1. Skymaps of point source statistical significance (normalised) for the ON–OFF source excess over a $\pm 1^{\circ}$ field after application of all cuts (table 1). The tracking positions for each year's data differs by $\sim 0.34^{\circ}$.

dependent on source distance from the camera centre d, and $\sigma_{miss} = 0.09$ for all d. A *length* cut dependent upon source position is also applied. These cuts are all selected *a priori* using Monte Carlo simulations of the CANGAROO 3.8 metre telescope and camera, and provide a quality factor of ~ 4 at $\sim$40% gamma-ray cut efficiency for any point source located within a $\pm 1^{\circ}$ area. A full description of this analysis is given by [12].

A number of sites (point and extended, listed in table 1) within the W28 region were searched for TeV gamma-ray emission. The tracking position of 1994 data was PSR J1801$-$23 and that for 1995 was a radio position labelled 'A83', defined by [1]. Skymaps (normalised ON$-$OFF excess in sigma for a point source as a function of assumed source position) are presented in figure 1, and reveal no statistically significant excesses. Upper limits to the TeV gamma-ray flux at the 3σ level (listed in table 1) were calculated. For the extended source examples, the events satisfying the cuts at source positions within a radius of interest were summed for ON and OFF source data. A slightly different gamma-ray trigger efficiency was used for each year's data to account for a lower event rate in 1995 compared to 1994, and all results were normalised to a 1.5 TeV energy threshold (representing the energy at the half-maximum of the distribution of triggered energies).

MODEL COMPARISON

We make a comparison of the EGRET results (spectrum from [7]) and our upper limit for an extended source centred on A83 from 1994 data (the lowest of our extended source upper limits) with a model of the TeV gamma-ray flux due to the decay of neutral pions [8] in figure 2. The model flux will scale according to

TABLE 1. Summary of the 3σ flux upper limits from several sites/features within the W28 region.

Feature	Flux($\geq$ 1.5 TeV) ph cm^{-2} s^{-1}	
	1994 Data	1995 Data
Radio position A83[a]	$< 3.36 \times 10^{-12}$	$< 2.95 \times 10^{-12}$
Radio position A83[b]	$< 8.75 \times 10^{-12}$	$< 6.67 \times 10^{-12}$
PSR J1801−23[c]	$< 3.20 \times 10^{-12}$	$< 3.32 \times 10^{-12}$
Masers (E&F)[d]	$< 4.14 \times 10^{-12}$	$< 3.47 \times 10^{-12}$
3EGJ1800−2338[e]	$< 8.82 \times 10^{-12}$	$< 1.18 \times 10^{-11}$

a: Point source at radio position A83, defined by [1].

b: Extended source of radius 0.35° centred on A83.

c: Point source at pulsar position [5].

d: Point source at average position of the two strongest maser sites E and F [2].

e: Highest pointlike significance within EGRET 95% error circle (0.32°) [4].

$F_\gamma \propto \frac{E_t(10^{51}\mathrm{erg})\ n(\mathrm{cm}^{-3})}{d^2(\mathrm{kpc}^2)}$, where values of the total energy available for CR production, $E_t = 0.01 \rightarrow 0.1$, the distance to the remnant, $d = 1.8 \rightarrow 4.0$ kpc, and the density of ambient matter, $n = 1.3$ cm^{-3}, are published ranges. The results of scaling the model flux according to these range of values are defined by the hashed region in figure 2. Results when assuming a much higher matter density of $n = 20$ cm^{-3} in combination with favourable values of E_t and d are indicated by the thick dot-dashed line. A proton injection spectrum of -2.1 (differential) and cutoff energy 10^{14}eV has been used in the model, ie. consistent with shock acceleration. When assuming a high value of n, the model flux is able to meet the EGRET data without violating our upper limit.

DISCUSSION

A search for TeV gamma ray emission from the W28 region was carried out on data taken in 1994 and 1995 with the CANGAROO 3.8m telescope. No evidence for point-like or extended TeV γ-ray emission from a number of sites in the W28 region was found. We compare the lowest of our extended source upper limits to the predicted TeV gamma ray emission from π° decay. From figure 2, the EGRET flux may be accounted by π° decay gamma-rays alone, if we assume a high ambient matter density ($n \sim 20$ cm^{-3}). Such a density is possible for W28, given the presense of a nearby molecular cloud and maser emission. However, an accelerated electron component from bremsstrahlung and inverse Compton scattering may also contribute. Further studies of results at X-ray energies (for e.g. [13]), may hint at the level of such components. A more detailed investigation of model parameters including spectral cutoffs is underway.

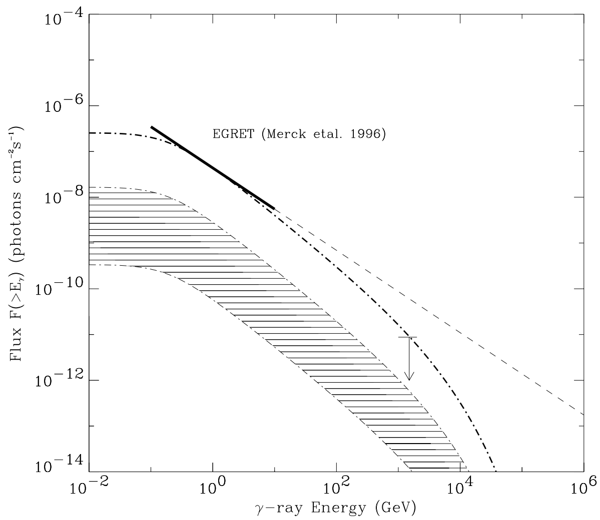

FIGURE 2. Comparison of our upper limit (extended source at A83 for 1994 data) and the EGRET flux of 3EG J1800−2338 [7] with a model predicting the TeV gamma-ray flux due to π° decay (hashed area and single dot-dashed line, [8]). See text for details.

ACKNOWLEDGEMENTS

This work is supported by a Grant-in-Aid in Scientific Research from the Japanese Ministry of Science, Sports and Culture, and also by the Australian Research Council. GR acknowledges the receipt of a JSPS postdoctoral fellowship.

REFERENCES

1. Andrews M.D. et al. 1983, *ApJ*, **266**, 684
2. Claussen M.J., Frail D.A., and Goss W.M. 1997, *ApJ* **489**, 143
3. Hara T. et al. 1993, *Nucl. Inst. Meth.*, **300**, A332
4. Hartman R.C. et al. 1999, *ApJ (Supp)*, **123**, 79
5. Kaspi A.G. et al. 1993, *ApJ*, **409**, L57
6. Long K.S., Blair W.P., White R.L. et al. 1991 *ApJ*, **373**, 567
7. Merck M. et al. 1996 *A & A*, **120**, 465
8. Naito T. and Takahara F. 1994 *J Phys G: Nucl Part. Phys.*, **20**, 477
9. Ong R.A. 1998 *Physics Reports*, **305**, 93
10. Rho J.H., Petre R., Pisarski R, and Jones L.R. 1996, *MPE Report*, **263**, 273
11. Romero G.E., Benaglia P. and Torres D.F., *A & A*, **348**, 868
12. Rowell G.P. et al. 1999, in preparation
13. Tomida H. et al. 1998, *Genshikaku Kenkyu*, **42**, 123, in japanese